えられた。

付　記

本論文の要旨は、第22回日本耳科学会総会・学術講演会（2012年10月、名古屋市）にてポスター発表した。

参考文献

1）Goto Y, Nonaka I, Horai S：A mutation in the tRNA$^{Leu(UUR)}$ gene associated with the MELAS subgroup of mitochondrial encephalomyopathies. Nature 348：651-653, 1990.

2）van den Ouweland JM, Lemkes HH, Ruitenbeek W, et al.：Mutation in mitochondrial tRNA$^{Leu(UUR)}$ gene in a large pedigree with maternally transmitted type II diabetes mellitus and deafness. Nat Genet 1：368-371, 1992.

3）Reardon W, Ross RJM, Sweeney MG, et al.：Diabetes mellitus associated with a pathogenic point mutation in mitochondrial DNA. Lancet 340：1376-1379, 1992.

4）Kato T, Nishigaki Y, Noguchi Y, et al.：Extensive and rapid screening for major mitochondrial DNA point mutations in patients with hereditary hearing loss. J Hum Genet 55：1-8, 2010.

5）Nussbaum RL, Mclnnes RR, Willard HF（福嶋義光監訳）：トンプソン&トンプソン　遺伝医学. メディカル・サイエンス・インターナショナル、東京、2009、pp. 156-159.

6）Schapira AH：Mitochondrial diseases. Lancet 379：1825-1834, 2012.

7）Kadowaki T, Kadowaki H, Mori Y, et al.：A subtype of diabetes mellitus associated with a mutation of mitochondrial DNA. N Engl J Med 330：962-968, 1994.

8）Sue CM, Lipsett LJ, Crimmins DS, et al.：Cochlear origin of sensorineural deafness in MELAS syndrome. Ann Neurol 43：350-359, 1998.

9）Jansen JJ, Maassen JA, van der Woude FJ, et al.：Mutation in mitochondrial tRNA$^{Leu(UUR)}$ gene associated with progressive kidney disease. J Am Soc Nephrol 8：1118-1124, 1997.

10）Fujii H, Mori Y, Kayamori K, et al.：A familial case of mitochondrial disease resembling Alport syndrome. Clin Exp Nephrol 12：159-163, 2008.

11）舩坂宗太郎、牛島達次郎、矢野　純：先天性キヌタ・アブミ関節離断症—発生学的ならびに臨床的考察による新名称の提案—. 日耳鼻 82：476-481, 1979.

12）舩坂宗太郎、牛島達次郎、矢野　純：外耳奇形を伴わない先天性耳小骨固着—その分類に関する提案—. 日耳鼻 82：793-798, 1979.

13）Otabe S, Sakura H, Shimokawa K, et al.：The high prevalence of the diabetic patients with a mutation in the mitochondrial gene in Japan. J Clin Endocrinol Metab 79：768-771, 1994.

14）Manwaring N, Jones MM, Wang JJ, et al.：Population prevalence of the MELAS A3243G mutation. Mitochondrion 7：230-233, 2007.

15）Elliott HR, Samuels DC, Eden JA, et al.：Pathogenic mitochondrial DNA mutations are common in the general population. Am J Hum Genet 83：254-260, 2008.

16）Nagata H, Kumahara K, Tomemori T, et al.：Frequency and clinical features of patients with sensorineural hearing loss associated with the A3243G mutation of the mitochondrial DNA in otorhinolaryngic clinics. J Hum Genet 46：595-599, 2001.

17）牧嶋知子、東　芳、中条恭子、他：外来の難聴患者におけるミトコンドリア遺伝子点変異. Audiol Jpn 44：54-59, 2001.

18）Usami S, Abe S, Akita J, et al.：Prevalence of mitochondrial gene mutations among hearing impaired patients. J Med Genet 37：38-40, 2000.

19）鈴木幹男、北西　剛、山名高世、他：難聴外来におけるミトコンドリア点変異の頻度. Otol Jpn 8：526-530, 1998.

20）Suzuki S, Oka Y, Kadowaki T, et al：Clinical features of diabetes mellitus with the mitochondrial DNA 3243 (A-G) mutation in Japanese: Maternal inheritance and mitochondria-related complications. Diabetes Res Clin Pract 59：207-217, 2003.

論文受付　24年11月16日
論文受理　25年3月12日

別刷請求先：〒113-8519　東京都文京区湯島1-5-45
東京医科歯科大学医学部耳鼻咽喉科　本田　圭司

Hearing Research 302 (2013) 26–31

Contents lists available at SciVerse ScienceDirect

Hearing Research

journal homepage: www.elsevier.com/locate/heares

Research paper

RNA analysis of inner ear cells from formalin fixed paraffin embedded (FFPE) archival human temporal bone section using laser microdissection – A technical report

Yurika Kimura [a,b,*], Sachiho Kubo [b], Hiroko Koda [c,d], Kazuhiro Shigemoto [b], Motoji Sawabe [e], Ken Kitamura [c]

[a] Department of Otolaryngology, Tokyo Metropolitan Geriatric Medical Hospital, 35-2, Sakae-cho, Itabashi, Tokyo 173 0015, Japan
[b] Research Team for Geriatric Medicine, Tokyo Metropolitan Institute of Gerontology, Sakae-cho, Itabashi, Tokyo, Japan
[c] Department of Otolaryngology, Graduate School, Tokyo Medical and Dental University, Yushima, Bunkyo, Tokyo, Japan
[d] Department of Otolaryngology, Ohkubo Hospital, Kabukicho, Shinjuku, Tokyo, Japan
[e] Section of Molecular Pathology, Graduate School of Health Care Sciences, Tokyo Medical and Dental University, Japan

ARTICLE INFO

Article history:
Received 1 January 2013
Received in revised form
16 April 2013
Accepted 22 April 2013
Available online 6 May 2013

ABSTRACT

Objective: Molecular analysis using archival human inner ear specimens is challenging because of the anatomical complexity, long-term fixation, and decalcification. However, this method may provide great benefit for elucidation of otological diseases. Here, we extracted mRNA for RT-PCR from tissues dissected from archival FFPE human inner ears by laser microdissection.

Methods: Three human temporal bones obtained at autopsy were fixed in formalin, decalcified by EDTA, and embedded in paraffin. The samples were isolated into spiral ligaments, outer hair cells, spiral ganglion cells, and stria vascularis by laser microdissection. RNA was extracted and heat-treated in 10 mM citrate buffer to remove the formalin-derived modification. To identify the sites where *COCH* and *SLC26A5* mRNA were expressed, semi-nested RT-PCR was performed. We also examined how long *COCH* mRNA could be amplified by semi-nested RT-PCR in archival temporal bone.

Results: *COCH* was expressed in the spiral ligament and stria vascularis. However, *SLC26A5* was expressed only in outer hair cells. The maximum base length of *COCH* mRNA amplified by RT-PCR was 98 bp in 1 case and 123 bp in 2 cases.

Conclusion: We detected *COCH* and *SLC26A5* mRNA in specific structures and cells of the inner ear from archival human temporal bone. Our innovative method using laser microdissection and semi-nested RT-PCR should advance future RNA study of human inner ear diseases.

1. Introduction

Mechanisms of sensorineural hearing loss have been analysed using advanced molecular techniques. Molecular genetic studies of experimental animals including mice have identified genes involved in deafness and have determined genotype–phenotype correlations (Gibson et al., 1995, Everett et al., 2001). However, molecular analysis using fixed and embedded human inner ear specimens has been challenging because they are usually inaccessible. While formalin-fixation and celloidin-embedding are standard histopathological methods for human temporal bone specimens, they are unsuitable for molecular analysis (Schuknecht, 1993). However, there are several reports in which DNA has been successfully extracted and analysed from human inner ear specimens. Genes involved in deafness were identified using a cDNA library from the human fetal inner ear (Robertson et al., 1998), and quantitative analysis of a mitochondrial DNA (mtDNA) mutation using archival temporal bones was reported (Takahashi et al., 2003, Koda et al., 2010). Recently, mitochondrial DNA deletions were

Abbreviations: FFPE, formalin fixed paraffin embedded; EDTA, ethylenediaminetetraacetic acid; mtDNA, mitochondrial DNA; LMD, laser microdissection; SV, stria vascularis; SGC, spiral ganglion cells; OHC, outer hair cells; SL, spiral ligament.

* Corresponding author. Department of Otolaryngology, Tokyo Metropolitan Geriatric Medical Hospital, 35-2, Sakae-cho, Itabashi, Tokyo 173 0015, Japan. Tel.: +81 3 3964 1141; fax: +81 3 3964 1982.
E-mail address: kimura@tmghig.jp (Y. Kimura).

0378-5955/$ – see front matter © 2013 Elsevier B.V. All rights reserved.
http://dx.doi.org/10.1016/j.heares.2013.04.008

detected in human inner ears from patients with presbycusis by laser microdissection (Markaryan et al., 2009).

In contrast to DNA analysis, RNA expression analysis can demonstrate the spatio-temporal activities of gene transcription and expression in tissues, providing important physiological and pathological information. Further, mRNA analysis is important because it examines the "working copy" of a gene. Therefore, studying mRNA extracted from human inner ears can provide further information concerning the molecular mechanisms of inner ear disorders of humans. Previously, we established an optimal method of extracting mRNA suitable for molecular biological applications from the autopsy specimens of human temporal bones (Kimura et al., 2007). However, this method uses frozen whole cochlea, and can not be applied to the retrospective analyses using formalin-fixed archival temporal bone specimens.

The objective of this study was to establish an optimal method of RNA expression analysis of specific sites in the human inner ear using archival (stored) FFPE human inner ear specimens and the laser microdissection techniques.

2. Materials and methods

2.1. Temporal bones

Three human temporal bones from individuals with no hearing impairment according to nursing records were obtained at autopsy. The cases were 2 males and 1 female of 70, 71, and 71 years of age, respectively. The post-mortem time before autopsy ranged from 1 to 15 h. The temporal bones were fixed in buffered 20% formalin at room temperature for 12–20 months, followed by decalcification in 10% ethylenediaminetetraacetic acid (EDTA) for 6–9 months at room temperature. After decalcification, the specimens, including the bony labyrinth, was cropped to a cube measuring 15 mm to fit standard plastic cassettes and glass slides. The specimens were embedded in paraffin, serially cut into 6 μm-thick thin sections, and mounted on a membrane slide for laser microdissection.

2.2. Laser microdissection

After deparaffinization of the thin sections by xylene and staining with toluidine blue, the spiral ligaments, spiral ganglion cells, stria vascularis, and outer hair cells in the basal turn were isolated using a laser microdissection system (Leica AS LMD; Wetzlar, Germany). This system uses a UV laser to isolate microscopic regions from samples. Tissue fragments from 3 successive sections of inner ear were placed gently into 0.5 ml microtubes filled with 50 μl tissue lysis buffer. The specimens were not touched, which makes specimen collection by gravity a contamination-free procedure.

2.3. RNA extraction

RNA extraction and cDNA synthesis was performed using the methods described by Hamatani et al. (2006). RNA was isolated from the microdissected tissue using the High Pure RNA Paraffin Kit (Roche Diagnostics; Basel, Switzerland) according to the manufacturer's protocols with some modifications. Briefly, microdissected tissue was digested with proteinase K at 55 °C overnight, followed by DNase I treatment. After the lysate was purified by the High Pure filter, RNA was eluted twice with 100 μl of RNase-free water. RNA was then precipitated by ethanol in the presence of 2 μl of ethachinmate (Nippon Gene; Tokyo, Japan), which is a carrier solution for the alcohol precipitation of DNA and RNA and resuspended in 30 μl of RNase-free water. The concentration of RNA was measured by absorption at 260 nm with GeneQuant 1300 (GE Healthcare UK Ltd; Buckinghamshire, England).

2.4. Heat treatment of RNA

Approximately 150 ng of total RNA was heated in 250 μl of 10 mM citrate buffer pH 4.0 at 70 °C for 45 min. After 25 μl sodium acetate was added into the solution, RNA was precipitated by ethanol in the presence of ethachinmate as a carrier, dried, and dissolved in RNase-free water to the final concentration of 10 ng/μl.

2.5. cDNA synthesis

The 11 μl of RNase-free solution containing 90 ng of total RNA and 50 pmol/ml of random primers was heated at 65 °C for 10 min and chilled in ice water. A mixture consisting of 4 μl of 5 × RT buffer, 2 μl of 20 mM DTT, 1 μl of 10 mM dNTPs, 1 μl of RNase Inhibitor (10 U/μl), and 1 μl of ReverTra Ace (Toyobo, Osaka, Japan) was added to the RNA solution and incubated at 42 °C for 60 min and at 70 °C for 15 min.

2.6. RT-PCR of COCH and SLC26A5 mRNA

We selected *COCH* and *SLC26A5* as the target genes for RT-PCR because cochlin, coded by *COCH* (accession No. NM_001135058), is the protein expressed most commonly in the inner ear other than collagen, and prestin, coded by *SLC26A5* (accession No. NG_023055) is a motor protein expressed specifically in outer hair cells. *GAPDH* (accession No.NG_007073), a typical house-keeping gene, was used for standardization. In order to detect very small amounts of target cDNA and to reduce the contamination in products due to the amplification of unexpected primer binding sites, semi-nested RT-PCR was performed. Forward and reverse primers were designed to cover different exons and introns to prevent a carry-on of the genomic DNA, in order not to detect a carry-on of genomic DNA using the free program on the internet, Primer 3 (http://primer3.sourceforge.net/). Primer sequences are shown in Table 1.

First RT-PCR was performed in a 20 μl volume containing 10 μl Premix Taq® (Takara Bio, Otsu, Japan), 0.5 μM of each specific primer and 1 μl of cDNA from the RT reaction. After an initial incubation at 94 °C for 3 min, the reaction mixtures were subjected to 30 cycles of amplification using the following sequence: 94 °C for 30 s, 55 °C for 30 s, and 72 °C for 45 s. This was followed by a final extension step at 72 °C for 7 min. The second RT-PCR was carried out in a 20 μl mixture containing 10 μl Premix Taq®, 0.5 μM of each specific primer and 1 μl of 9× first RT-PCR product following the same sequence of the first RT-PCR. Finally, 8 μl of the reaction mixture was run on a 3% agarose gel and visualized with ethidium bromide.

2.7. RT-PCR of COCH with different sizes of PCR products

To elucidate how long mRNA could be preserved in very small samples microdissected from formalin-fixed, long-term EDTA-decalcified, and paraffin-embedded thin sections, cDNA of *COCH* from the specimens of the spiral ligament was amplified using 5 sets of primers that would yield PCR products of different sizes from 98 to 180 bp as shown in Tables 2 and 3, and Fig. 1, with the second PCR product size of 87 bp.

Table 1
Primer sequences and product sizes for semi-nested RT-PCR of *COCH*, *SLC26A5*, and *GAPDH* mRNA.

mRNA	Forward primer	Reverse primer for the first PCR	Reverse primer for the second PCR	Product size of the first PCR	Product size of the second PCR
COCH	GGCATCCAGTCTCAAATGCT	GTGCTGTGGACACTGCTTGT	GTCCTGTGGCCTCCTGTGTA	103	85
SLC26A5	GTCTCGAAGCCTTGTTCAGG	GGGCAATGATTCAAAGAGGA	GGAAGACACAGCTTGCAGGT	118	86
GAPDH	AATGACCCCTTCATTGACCTC	ATGGGATTTCCATTGATGACA	TTCCATTGATGACAAGCTTCC	122	115

2.8. Ethical considerations

Consent for using temporal bone tissues removed at autopsy was obtained from the patients' relatives. The present study was approved by the Ethical Review Board at Tokyo Metropolitan Geriatric Medical Hospital, pursuant to Article 18 of the Cadaver Autopsy and Preservation Act.

3. Results

3.1. Laser microdissection

The microdissected areas in the cochlea are shown in Fig. 2. The outer hair cells, spiral ganglion cells, the stria vascularis, and the spiral ligament were dissected separately.

3.2. Site-specific expression of COCH and SLC26A5 in the cochlea

The results of *COCH* and *SLC26A5* site-specific expression are shown in Figs. 3 and 4. *COCH* expression was detected only in the spiral ligament and the stria vascularis, and *SCL26A5* was expressed in the outer hair cells only. *GAPDH* expression was detected in all of the structures examined.

3.3. RT-PCR of COCH with different sizes of PCR products

The maximum length of PCR amplicons for the first RT-PCR was 98 bp in 1 case and was 123 bp in 2 cases in each experiment (Fig. 5). These results suggest that approximately 100 bp was the maximum preserved length of mRNA after the long-term successive processing of formalin fixation, EDTA decalcification, and paraffin embedding.

Table 2
Primer sequences for semi-nested RT-PCR of *COCH* mRNA.

	Primer codes	Primer sequences
Forward primer	F	CAC ATG TGG GCC TTG TTC AA
Reverse primer	R1	CAA ACA AAA CAT CTT TGG CTG A
	R2	TTC CTT TAT GGC AAA CAA AAC A
	R3	TGG AAT TAC CCC CTC TGA AA
	R4	TGC TTC AAG GCT TTT CCT GT
	R5	CCG TGA AGA ATT TCT GAG CA
	R6	CTC CAG CAT CTA CCG TGA AG

Table 3
The product sizes of semi-nested RT-PCR of *COCH* mRNA.

Primer combination of first PCR	Product size of first PCR (bp)	Primer combination of second PCR	Product size of second PCR (bp)
F-R2	98	F-R1	87
F-R3	123		
F-R4	145		
F-R5	168		
F-R6	180		

The primer codes are defined in Table 2.

4. Discussion

We have successfully optimized a semi-nested RT-PCR method of detecting *COCH* and *SLC25A5* expression from specific sites of the inner ear using archival FFPE human inner ear specimens and the laser microdissection techniques. The maximal size of the *COCH* PCR amplicons was 98 bp and 123 bp.

4.1. DNA study of inner ears

Wackym et al. reported the first molecular analysis of human temporal bone pathology in 1993 (Wackym et al., 1993). However, DNA analysis of the whole section, as in their method, is of limited value because the inner ear is composed of heterogeneous and highly differentiated cells. Laser microdissection is a useful tool that allows the combination of morphological analysis and molecular biological analysis. We introduced this method for mitochondrial DNA analysis in the human temporal bone for the first time (Kimura et al., 2005), and elucidated a correlation between the mtDNA mutation rate and atrophy of the stria vascularis, as well as decreases in spiral ganglion cells (Koda et al., 2010). Markaryan et al. reported a large scale deletion of mtDNA in the cochlea and showed that major arc mtDNA deletions contributed to the observed deficit in *COX3* expression (Markaryan et al., 2009). These results suggest a correlation between presbycusis and the deletion of mtDNA in the cochlea.

4.2. mRNA expression study of the inner ear

Although DNA analysis using the laser microdissection method has become established to some degree, gene expression analysis of targeted mRNA remains challenging because RNA is more susceptible to strand breakage and cross linking by formalin fixation than DNA after fixation and decalcification (Chung and Hewitt, 2010). To overcome this difficulty, several research groups have attempted RNA analysis of archival human temporal bones. Lee et al. reported the first study of RT-PCR for archival temporal bones in 1997, in which they examined the expression of the γ-actin gene (Lee et al., 1997). In their report, the expression of γ-actin mRNA was detected in only one of ten archival temporal bone specimens, and the authors concluded that the analysis of gene expression from an archival section was very limited because the mRNA had been degraded by RNases. Lin et al. reported the RNA analysis of temporal bone soft tissues (Lin et al., 1999). They harvested temporal bones at immediate autopsies and showed the manifestations and

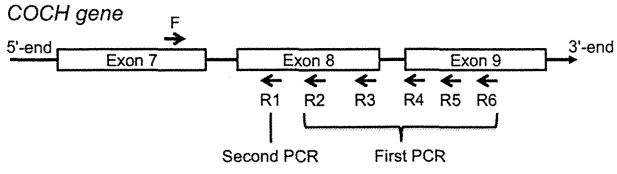

Fig. 1. Positions of forward and reverse primers that were used to elucidate the maximum preserved size of mRNA in the *COCH* gene. Forward and reverse primers were designed to cover different exons and introns and not to detect a carry-on of genomic DNA.

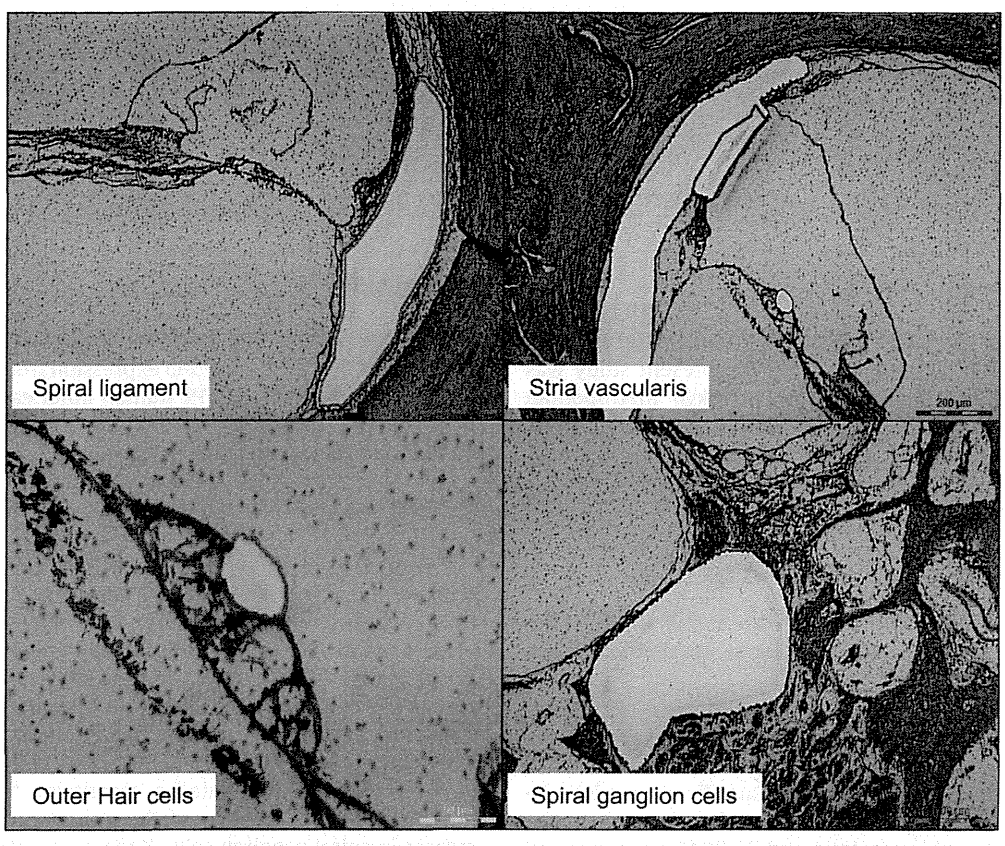

Fig. 2. Histological images of the spiral ligament, spiral ganglion cells, the stria vascularis and outer hair cells in the basal turn of the inner ear. After deparaffinization of the thin sections by xylene and staining with toluidine blue, the spiral ligaments, spiral ganglion cells, stria vascularis, and outer hair cells in the basal turn were isolated using a laser microdissection system (Leica AS LMD; Wetzlar, Germany). All microdissected tissue fragments from 3 successive tissue sections were collected into 0.5 ml microtubes filled with 50 µl tissue lysis buffer.

localizations of mRNA of mucin genes, such as *MUC5B* and *MUC1*, in the submucosal gland of the Eustachian tube and the middle ear. They suggested a high possibility of RNA analysis within 6 h of death. Under clinical circumstances, however, it is not realistic to harvest a temporal bone in 6 h after death. We developed a method of detection of *COCH* mRNA expression, as well as *GAPDH* mRNA expression using RNA extracted from membranous labyrinths dissected from formalin-fixed or frozen human cochlea (Kimura et al., 2007). This method is useful because removal of temporal bone specimens could be incorporated into the protocol of a conventional autopsy. However, this method was not able to utilize archival sections effectively. Hall et al. reported optimization of RNA detection from archival guinea pig temporal bones by the Trizol extraction method (Hall et al., 2007). This approach may be useful,

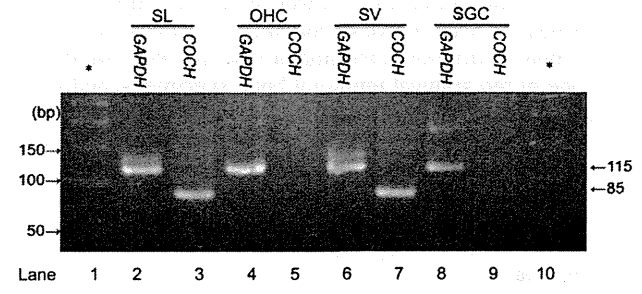

Fig. 3. Optimized semi-nested RT-PCR analysis of *GAPDH* and *COCH* in the FFPE human cochlea. The length of amplicons of *GAPDH* and *COCH* is 85 bp and 115 bp. Lane 1 and 10 are 50 bp ladder markers (asterisks(*)). Lane 2 and 3, semi-nested RT-PCR results from the spiral ligament(SL) using primers to GAPDH and COCH. Lane 4 and 5, semi-nested RT-PCR results from outer hair cells (OHC) using primers to GAPDH and COCH. Lane 6 and 7, semi-nested RT-PCR results from the stria vascularis (SV) using primers to GAPDH and COCH. Lane 8 and 9, semi-nested RT-PCR results from the spiral ganglion cells (SGC) using primers to GAPDH and COCH. Universal expression of *GAPDH* is noted. *COCH* is expressed in the spiral ligament and the stria vascularis, but is not expressed in the outer hair cells and spiral ganglion cells.

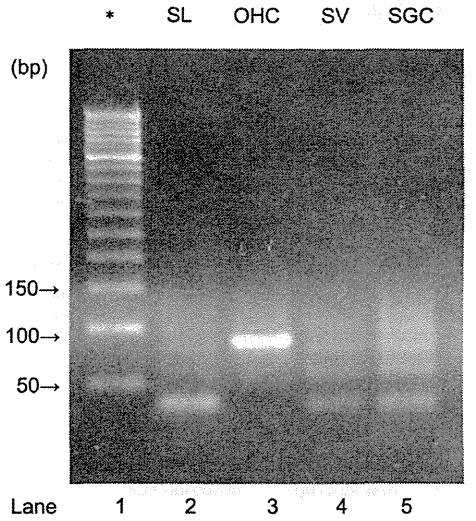

Fig. 4. Optimized semi-nested RT-PCR analysis of *SLC26A5* in the FFPE human cochlea. The length of the amplicon of *SLC26A5* is 86 bp. Lane 1 is 50 bp ladder markers (an asterisk(*)). Lane 2 to 5, semi-nested RT-PCR results from the spiral ligament(SL), the outer hair cells (OHC), the stria vascularis (SV) and spiral ganglion cells (SGC) using primers to *SLC26A5*. *SLC26A5* is expressed in the outer hair cells, but is not expressed in the spiral ligament, the stria vascularis, and the spiral ganglion cells.

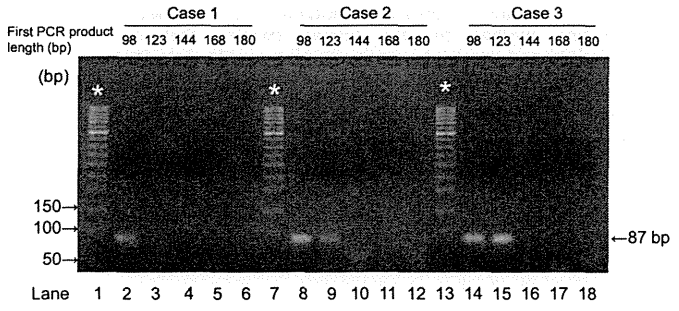

Fig. 5. Optimized semi-nested RT-PCR analysis of *COCH* to elucidate the maximum preserved length of mRNA extracted from FFPE human cochlea by using different reverse primers in first RT-PCR. Lane 1, 7 and 13 are 50 bp ladder markers (asterisks(*)). Lane 2 to 6, semi nested RT-PCR of *COCH* of the stria vascularis of case 1. Lane 8 to 12, semi nested RT-PCR of *COCH* of the stria vascularis of case 2. Lane 14 to 18, semi nested RT-PCR of *COCH* of the stria vascularis of case 3. Lane 2, 8 and 14 are the semi nested RT-PCR products of which first RT-PCR product length is 98 bp. Lane 3, 9 and 15 are the semi nested RT-PCR products of which first RT-PCR product length is 123 bp. Lane 4, 10 and 16 is the semi nested RT-PCR product of which first RT-PCR product length is 144 bp. Lane 5, 11 and 17 are the semi nested RT-PCR products of which first RT-PCR product length is 168 bp. Lane 6, 12 and 18 are the semi nested RT-PCR products of which first RT-PCR product length is 180 bp. The length of semi-nested PCR products is 87 bp. Up to 123 bp can be preserved in two cases and up to 98 bp in one case.

but it is not clear that this method could be applied to human archival inner ear specimens dissected by laser microdissection because, in their study, whole sections of the temporal bone were used and the period of fixation and decalcification was much shorter than those used for human samples.

4.3. mRNA expression study using tiny tissue samples that were laser-microdissected from archival human FFPE temporal bone

Pagedar et al. were the first to succeed in the analysis of RNA of the human inner ear from FFPE tissue using laser capture microdissection (Pagedar et al., 2006). They examined the vestibular organ dissected from a temporal bone block before fixation, and not archival cochlea samples. Therefore, our trial to extract mRNA from laser microdissected tissue (outer hair cells, the stria vascularis, spiral ganglion cells, and the spiral ligament) of human archival FFPE temporal bone sections was extremely challenging. Hamatani et al. indicated that RT-PCR amplification of degraded RNA extracted from archival unbuffered formalin-fixed, paraffin-embedded thyroid cancer tissue samples, which were preserved at room temperature for 19–21 years, could be improved by heating RNA in citrate buffer prior to cDNA synthesis (Hamatani et al., 2006). Since FFPE-derived RNA is degenerated into very short fragments and chemically modified, and reverse transcription from polyA tail is inefficient, the use of random primers instead of Oligo dT primers was recommended for cDNA synthesis (Farragher et al., 2008). Using these ideas and semi-nested PCR enabled us to amplify extremely small amounts of nucleic acid, and to extract mRNA from laser microdissected tissue of human archival FFPE temporal bone sections. Hamatani et al. reported that longer fragments up to 250 bp in the preheated RNA could be amplified in all cases compared with the non-treated RNA (Hamatani et al., 2006), while only very short fragments of RNA of approximately 100 bp could be obtained in our study. The fragmentation of the RNA strands could be ascribed to different tested organs (temporal bone in our study vs. thyroid tissue in their study), longer formalin fixation-period, and long-term decalcification in our study. These disadvantages, such as a long-period of formalin fixation and decalcification, influence the preservation of morphology such as shrinkage of tissue. Takahashi et al. reported excellent immunostaining results for the human cochlea, such as immunostaining for prestin in the cytoplasm of the human outer hair cells (Takahashi et al., 2010). We consider that the complementary use of molecular and immunohistochemical techniques will become a valuable tool for future study of the human inner ear.

5. Conclusions

Although molecular analysis using human inner ear specimens is challenging because of the anatomical complexity and long-term fixation and decalcification, it can provide significant data for the elucidation of otological disorders. We extracted mRNA from archival FFPE human inner ears by laser microdissection, and detected site-specific *COCH and SLC26A5* mRNA expression by RT-PCR from archival human temporal bones. We hope our innovative methods will pave the way for future RNA analyses of human inner ear disease.

Acknowledgements

This study was supported by Grants-in-Aid for Scientific Research (Nos. 19791250, 21390459, 22659305, 23791953) from the Ministry of Education, Culture, Sports, Science and Technology, Japan. The authors wish to thank Mr Goto, Mr Mukaiyama, Ms Hasegawa, and all other technicians in the Departments of Pathology of Tokyo Metropolitan Geriatric Hospital for their excellent pathological work. We also express our sincere gratitude to the deceased whose temporal bones contributed to this study.

References

Chung, J.Y., Hewitt, S.M., 2010. An optimized RNA extraction method from archival formalin-fixed paraffin-embedded tissue. Methods Mol. Biol. 611, 19–27.
Everett, L.A., Belyantseva, I.A., Noben-Trauth, K., Cantos, R., Chen, A., Thakkar, S.I., Hoogstraten-Miller, S.L., Kachar, B., Wu, D.K., Green, E.D., 2001. Targeted disruption of mouse Pds provides insight about the inner-ear defects encountered in Pendred syndrome. Hum. Mol. Genet. 10, 153–161.
Farragher, S.M., Tanney, A., Kennedy, R.D., Harkin, P.D., 2008. RNA expression analysis from formalin fixed paraffin embedded tissues. Histochem. Cell. Biol. 130, 435–445.
Gibson, F., Walsh, J., Mburu, P., Varela, A., Brown, K.A., Antonio, M., Beisel, K.W., Steel, K.P., Brown, S.D., 1995. A type VII myosin encoded by the mouse deafness gene shaker-1. Nature 374, 62–64.
Hall, K.L., Pitts, D.R., Anne, S., Semaan, M.T., Alagramam, K.N., Megerian, C.A., 2007. Optimization of ribonucleic acid detection from archival Guinea pig temporal bone specimens. Otol Neurotol. 28, 116–123.
Hamatani, K., Eguchi, H., Takahashi, K., Koyama, K., Mukai, M., Ito, R., Taga, M., Yasui, W., Nakachi, K., 2006. Improved RT-PCR amplification for molecular analyses with long-term preserved formalin-fixed, paraffin-embedded tissue specimens. J. Histochem. Cytochem. 54 (7), 773–780.
Kimura, Y., Kouda, H., Kobayashi, D., Suzuki, Y., Ishige, I., Iino, Y., Kitamura, K., 2005. Detection of mitochondrial DNA from human inner ear using real-time polymerase chain reaction and laser microdissection. Acta Otolaryngol. 125, 697–701.
Kimura, Y., Kubo, S., Koda, H., Noguchi, Y., Sawabe, M., Maruyama, N., Kitamura, K., 2007. Quantitative analysis of mRNA in human temporal bones. Acta Otolaryngol. 127 (10), 1024–1030.
Koda, H., Kimura, Y., Ishige, I., Eishi, Y., Iino, Y., Kitamura, K., 2010. Quantitative cellular level analysis of mitochondrial DNA 3243A>G mutations in individual tissues from the archival temporal bones of a MELAS patient. Acta Otolaryngol. 130 (3), 344–350.
Lee, K.H., McKenna, M.J., Sewell, W.F., Ung, F., 1997. Ribonucleases may limit recovery of ribonucleic acids from archival human temporal bones. Laryngoscope 107, 1228–1234.
Lin, J., Kawano, H., Paparella, M.M., Ho, S.B., 1999. Improved RNA analysis for immediate autopsy of temporal bone soft tissues. Acta Otolaryngol. 119, 787–795.
Markaryan, A., Nelson, E.G., Hinojosa, R., 2009. Quantification of the mitochondrial DNA common deletion in presbycusis. Laryngoscope 119, 1184–1189.
Pagedar, N.A., Wang, W., Chen, D.H., Davis, R.R., Lopez, I., Wright, C.G., Alagramam, K.N., 2006. Gene expression analysis of distinct populations of cells isolated from mouse and human inner ear FFPE tissue using laser capture microdissection–a technical report based on preliminary findings. Brain Res. 1091 (1), 289–299.
Robertson, N.G., Lu, L., Heller, S., Merchant, S.N., Eavey, R.D., McKenna, M., Nadol Jr., J.B., Miyamoto, R.T., Linthicum Jr., F.H., Lubianca Neto, J.F., Hudspeth, A.J., Seidman, C.E., Morton, C.C., Seidman, J.G., 1998. Mutations in a

novel cochlear gene cause DFNA9, a human nonsyndromic deafness with vestibular dysfunction. Nat. Genet. 20, 299–303.
Schuknecht, H., 1993. Pathology of the Ear, second ed. Lea & Febiger, Philadelphia.
Takahashi, K., Merchant, S.N., Miyazawa, T., Yamaguchi, T., McKenna, M.J., Kouda, H., Iino, Y., Someya, T., Tamagawa, Y., Takiyama, Y., Nakano, I., Saito, K., Boyer, P., Kitamura, K., 2003. Temporal bone histopathological and quantitative analysis of mitochondrial DNA in MELAS. Laryngoscope 113, 1362–1368.
Takahashi, M., Kimura, Y., Sawabe, M., Kitamura, K., 2010. Modified paraffin-embedding method for the human cochlea that reveals a fine morphology and excellent immunostaining results. Acta Otolaryngol. 130, 788–792.
Wackym, P.A., Simpson, T.A., Gantz, B.J., Smith, R.J., 1993. Polymerase chain reaction amplification of DNA from archival celloidin-embedded human temporal bone sections. Laryngoscope 103, 583–589.

Annals of human genetics

doi: 10.1111/ahg.12053

A *DFNA5* Mutation Identified in Japanese Families with Autosomal Dominant Hereditary Hearing Loss

Ayako Nishio[1], Yoshihiro Noguchi[1]*, Tatsuya Sato[1], Taeko K. Naruse[2], Akinori Kimura[2], Akira Takagi[3] and Ken Kitamura[1]

[1]*Department of Otolaryngology, Tokyo Medical and Dental University, Tokyo, Japan*
[2]*Department of Molecular Pathogenesis, Medical Research Institute, Tokyo Medical and Dental University, Tokyo, Japan*
[3]*Department of Otorhinolaryngology, Head and Neck Surgery, Shizuoka General Hospital, Shizuoka, Japan*

Summary

Mutations in *DFNA5* lead to autosomal dominant nonsyndromic hereditary hearing loss (NSHHL). To date, four different mutations in *DFNA5* have been reported to cause hearing loss. A 3 bp deletion mutation (c.991-15_991-13del) was identified in Chinese and Korean families with autosomal dominant NSHHL, which suggested that the 3 bp deletion mutation was derived from a single origin. In the present study, we performed genetic screening of mutations in the interval between intron 6 and exon 9 of *DFNA5* in 65 Japanese patients with autosomal dominant NSHHL and identified the c.991-15_991-13del mutation in two patients. Furthermore, we compared the DFNA5-linked haplotypes consisting of intragenic SNPs between the reported Chinese and Korean families and found that the Japanese patients showed a shared region spanning 41,874 bp. This is the first report of *DFNA5* mutations in Japanese patients with autosomal dominant NSHHL, supporting the suggestion that the 3 bp deletion mutation occurred in their ancestors.

Keywords: DFNA5, autosomal dominant, hereditary, hearing loss, sensorineural, nystagmus

Introduction

Hearing loss (HL) is the most common birth defect and the most prevalent sensory disorder (Hilgert et al., 2009; Ito et al., 2010; Korver et al., 2011). Bilateral congenital HL occurs in 1.86 per 1000 newborns (Morton & Nance, 2006). Hereditary HL accounts for at least two-thirds of cases of congenital HL. Among patients with hereditary HL, 70% exhibit nonsyndromic hereditary HL (NSHHL). Hereditary patterns subdivide the NSHHL into the autosomal dominant type (DFNA), autosomal recessive type (DFNB), X-linked type (DFNX), and maternally inherited type associated with mitochondrial DNA mutations. DFNA accounts for 20%–25% of cases of NSHHL and is usually recognized to be a postlingual progressive form of HL (Van Camp et al., 1997). Thus far, more than 60 DFNA loci have been mapped, among which 27 causative genes have been identified [The Hereditary Hearing Loss Homepage (http://hereditaryhearingloss.org/)].

*Corresponding author: Yoshihiro Noguchi, Department of Otolaryngology, Tokyo Medical and Dental University, 1-5-45, Yushima, Bunkyo-ku, Tokyo 113-8519, Japan. Tel: +81 3 5803 5308; Fax: +81 3 3813 2134; E-mail: noguchi.oto@gmail.com

DFNA5 (OMIM# 600994 is caused by mutations in *DFNA5*, which was first identified in an extended Dutch family with autosomal dominant NSHHL (Van Camp et al., 1995; Van Laer et al., 1998). To date, four different mutations in *DFNA5* have been reported to cause HL (Van Laer et al., 1998; Yu et al., 2003; Bischoff et al., 2004; Cheng et al., 2007). All four mutations are located in introns 7 or 8, and are expected to lead to skipping of exon 8, resulting in a frameshift, and presumably causing premature truncation of the DFNA5 protein. On the other hand, a mouse mutant with a targeted deletion of exon 8 of *Dfna5* does not show HL (Van Laer et al., 2005). Furthermore, a frameshift mutation in exon 5 of *DFNA5* that would truncate the protein did not cosegregate with NSHHL in an Iranian family (Van Laer et al., 2007). These observations suggest that *DFNA5*-associated HL represents a mechanism of gain-of-function, and not haploinsufficiency.

Park et al. (2010) detected a c.991-15_991-13del mutation in a Korean family, which was identical to the mutation previously reported in a Chinese family (Yu et al., 2003). An analysis of *DFNA5* mutation-linked haplotypes between the Chinese and Korean patients suggested that the 3 bp deletion mutation was derived from a single origin (Park et al., 2010).

Although no DFNA5 families have been reported in Japan, it is possible that mutations in *DFNA5* exist in Japanese patients with autosomal dominant NSHHL. In the present study, we performed genetic screening of *DFNA5* mutations in the interval between intron 6 and exon 9 in Japanese patients with autosomal dominant NSHHL.

Materials and Methods

Patients

All procedures were approved by the Ethics Reviewing Committee of Tokyo Medical and Dental University and were carried out after obtaining written informed consent from each individual and/or the parents of the children.

We enrolled 65 unrelated Japanese patients with autosomal dominant NSHHL. Inheritance patterns were presumed based on the family pedigrees: at least one patient with HL was found in each generation. The patient population consisted of 39 females and 26 males between 12 and 82 years of age (mean ± standard deviation: 42.9 ± 17.1 years). After performing physical and otoscopic examinations, pure-tone audiometry was carried out in all patients. All patients suffered from bilateral sensorineural HL. The pure-tone average (PTA) calculated from audiometric thresholds at 500, 1000, 2000, and 4000 Hz ranged from 15.0 to 115.0 dB (mean ± standard deviation: 50.9 ± 19.4 dB). The severity of HL was categorized as follows: mild (PTA $\leq$ 40 dB) in 19 patients, moderate (40 dB < PTA $\leq$ 70 dB) in 38 patients, severe (70 dB < PTA $\leq$ 90dB) in four patients, and profound (90 dB < PTA) in four patients. The audiometric configurations (Mazzoli et al., 2003) included the high-frequency form in 27 patients, the low-frequency ascending form in 13 patients, the mid-frequency U-shaped form in six patients, the flat form in eight patients, and the other forms in 11 patients.

Mutation Screening

Genomic DNA was extracted from peripheral blood using standard methods. Exons 7–9 and introns 6–8 of *DFNA5* were amplified by polymerase chain reaction (PCR) in a thermal cycler (model 9700; Life Technologies, Carlsbad, CA, USA). Primers were designed using the GENETYX software program (Genetyx Corporation, Tokyo, Japan) to amplify the whole region of approximately 7700 bp and to sequence segmentalized regions of 600–700 bp. The sequences of the primers used in this study are listed in Table S1. The PCR reaction mixture (20 μL) contained 20 ng of DNA, 0.5 μmol/L of primers, and 1.0 U of LA Taq DNA polymerase (Takara, Shiga, Japan). The cycling protocol included an initial 1 min of denaturation at 94°C, followed by 30 step cycles of 98°C for 10 s and 68°C for 10 min, with a final step of 10 min at 72°C. The PCR products were purified using a QIAquick PCR purification Kit (Qiagen, Hilden, Germany) according to the manufacturer's instructions and were directly sequenced on both strands using an ABI Prism Big Dye Terminator Cycle Sequencing Ready Kit (Life Technologies Corp.) on an ABI Prism model 3130×l or 310 Genetic Analyzer.

Genetic Analysis of the Proband Patient and Family Members with a Mutation

When a mutation was detected in a patient, amplification and direct sequencing were conducted for all coding regions and exon–intron boundaries of *DFNA5*. The presence of a mutation was analyzed in 100 unrelated healthy Japanese subjects with normal hearing. A genetic analysis of the *GJB2* mutation and mitochondrial DNA 1555A > G mutation was performed to exclude the most frequent cause of NSHHL. The coding region and exon–intron boundaries of *GJB2* were amplified using the following primers: GJB2-1F 5′-TGC TTG CTT ACC CAG ACT CA-3′, GJB2-1R 5′-TGG GAG ATG GGG AAG TAG TG-3′; GJB2-2F 5′-TAC GAT CAC TAC TTC CCC ATC TC-3′, GJB2-2R 5′-GCA ATC ATG AAC ACT GTG AAG AC-3′; GJB2-3F 5′-TGG TGG ACC TAC ACA AGC AG-3′, GJB2-3R 5′-CCT CAT CCC TCT CAT GCT GT-3′. Forward (5′-AAA GAC GTT AGG TCA AGG TG-3′) and reverse (5′-GCT ACA TAG ACG GGT GTG CTC-3′) primers were used to amplify mitochondrial DNA *MTRNR1* including position 1555.

Four fluorescent-labeled microsatellite markers (D7S2525, D7S1791, G10542, and D7S2458) flanking the *DFNA5* gene, which were used in a previous paper (Park et al., 2010), were genotyped in the family members of the proband patients with a mutation (Table S1). In the PCR amplifications, the reaction mixture (25 μL) contained 20 ng of DNA, 0.2 μmol/L of primers, and 1.0 U of FastStart Taq DNA polymerase (Roche Applied Science, Mannheim, Germany). The cycling protocol included an initial 4 min of denaturation at 95°C, followed by 35 step cycles of 95°C for 30 s, 55°C for 30 s, and 72°C for 1 min, with a final elongation step of 7 min at 72°C. The PCR products were analyzed using GeneScan 500 LIZ size standard (Applied Biosystems, Santa Clara, CA, USA) on an ABI Prism model 3130×l Genetic Analyzer. The GeneMapper software program (Applied Biosystems) was used to analyze the resulting data.

Haplotype Analysis

Twenty intragenic single-nucleotide polymorphisms (SNPs) of *DFNA5*, which were reported in a previous paper (Park

et al., 2010), were analyzed using PCR amplification and DNA sequencing in two unrelated patients with a mutation as well as in the family members of a patient. The mutation-linked haplotype in the Japanese patients was compared with that reported in Korean and Chinese patients with the identical mutation (Park et al., 2010).

The linkage disequilibrium (LD) structure of the region around *DFNA5* was investigated using the HapMap data (http://hapmap.ncbi.nlm.nih.gov/) for Japanese and Chinese, and expressed for r^2 and D' using the Haploview software program (Broad Institute, Cambridge, MA, USA).

Audiovestibular Examinations

Audiological examinations including speech audiometry, distortion-product otoacoustic emissions (DPOAEs), and auditory brainstem responses (ABRs) were conducted in the patients with a mutation and their family members. DPOAE, an objective inner ear test, was recorded and analyzed using an ILO292 analyzer (Otodynamics Ltd, Hatfield, Herts, UK).

The vestibular examinations included positional, positioning, and spontaneous nystagmus tests with an infrared charge-coupled device (CCD) camera. Air caloric testing was performed using electronystagmography (ENG). Caloric hypoplexia was defined as a maximal slow phase velocity (MSV) less than 20°/s.

Results

Screening for DFNA5 Mutations

In this study, we investigated sequence variations in an approximately 7700 bp region of *DFNA5* spanning from intron 6 to exon 9 (Fig. 1). Two of 65 patients (3.1%) carried a c.991-15_991-13del mutation, which was identical to the mutation reported in a Chinese family (Yu et al., 2003) and a Korean family (Park et al., 2010). The 3 bp deletion mutation was not detected in 100 healthy Japanese controls.

Among the other 37 variants detected in the patients, 24 were polymorphisms found on the HapMap Homepage (http://hapmap.ncbi.nlm.nih.gov/) and 1000 Genomes website (http://www.1000genomes.org/). The remaining 13 variants were detected in 100 Japanese controls and were therefore considered to be novel polymorphisms (Table S2).

Family Analysis

The family studies showed that one of the two patients with the 3 bp deletion mutation was from a five-generation family (TMDU244), while the other was from a three-generation family (TMDU313) (Fig. 2). No *GJB2* mutations, mitochondrial DNA 1555A > G mutation, or other mutations in any coding regions or exon–intron boundaries of *DFNA5* were detected in the two patients with the *DFNA5* mutation.

In the TMDU244 family, audiometric evaluations and blood DNA extractions were performed in 12 of the 35 family members (eight affected members and four unaffected members). All affected members carried the c.991-15_991-13del mutation, whereas three of the four unaffected members had no mutations and one member with normal hearing (V:10, a 22-year-old female) was found to harbor the mutation (Fig. S1). An analysis of microsatellite markers linked to the *DFNA5* locus found that the *DFNA5* mutation was linked to NSHHL (Fig. 2). Eight affected members exhibited bilateral symmetrical high-frequency sensorineural HL (Fig. S1). The onset of HL ranged from 10 to 30 years of age. The findings of DPOAE and ABR suggested the HL to be of cochlear origin. None of the family members had vestibular symptoms, and vestibular examinations showed no findings of gaze, positioning, or spontaneous nystagmus, although positional nystagmus was detected in two members (IV:7 and V:7). Caloric testing showed bilateral normal responses in IV:7 and bilateral slight hypoplexia in V:7.

In the TMDU313 family, an audiometric evaluation and genetic analysis were performed in the proband only (III:1). The proband had bilateral symmetrical high-frequency sensorineural HL (Fig. S1) without vestibular symptoms. The HL had started at 18 years of age and was progressive. The word recognition score was 75% in the right ear and 80% in the left ear. The findings of DPOAE and ABR suggested the HL to be of cochlear origin.

Haplotype Analysis

In order to gain insights into the origin of the mutation, we investigated 20 SNPs and four microsatellite markers linked to the *DFNA5* locus in the subjects from the TMDU244 family and the patient from the TMDU311 family (Fig. 1b, Table 1). A comparison of the *DFNA5* mutation-linked haplotypes in the TMDU244 family with those observed in Chinese (Yu et al., 2003) and Korean (Park et al., 2010) families revealed that the mutation-linked haplotypes shared an identical region of 41,874 bp spanning from rs2240005 to rs55926631. Quite interestingly, the TMDU313 patient was homozygous for the A > G variant (rs2269812), which was not found in the other families.

The LD structure of the 750 kb region around *DFNA5* was investigated using the HapMap data (Fig. S2). It was found that the analyzed region was in a large LD block, based on the D' plot data, although it could be subdivided into seven

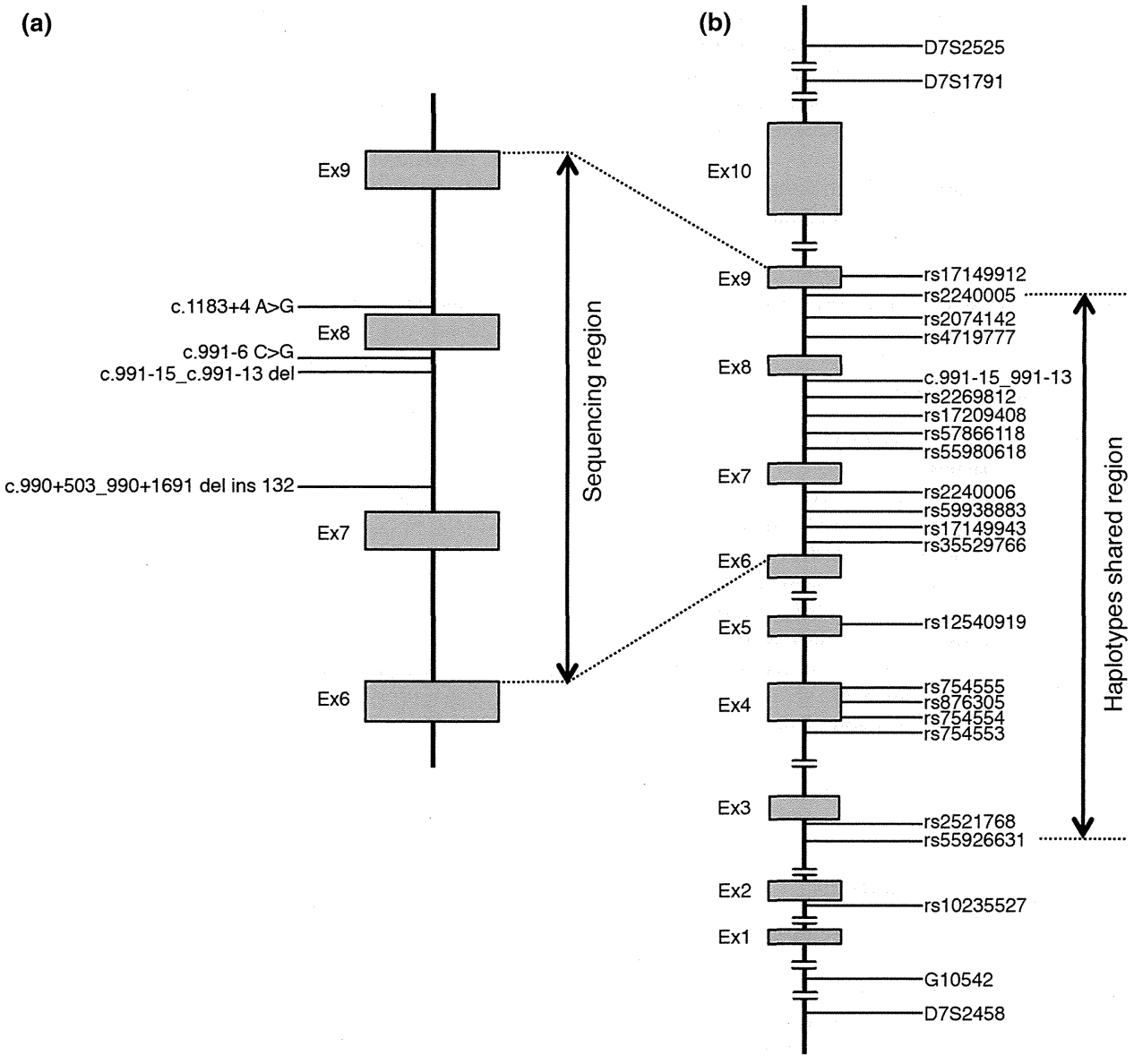

Figure 1 Physical map of human chromosome 7p15. A schematic diagram of *DFNA5* showing the locations of the four reported mutations and analyzed region in this study (a), as well as the shared region in the DFNA5 families (b).

strong LD blocks from block A to G, as deduced from the r^2 plot data. *DFNA5* was included in the LD block *D* of approximately 300 kb, which included *MPP6* and a part of *OSBPL3*.

Discussion

This is the first report of screening for *DFNA5* mutations among Japanese patients with autosomal dominant NSHHL. We detected a mutation, c.991-15_991-13del, in two patients, which was previously reported in East Asian families (Yu et al., 2003; Park et al., 2010). Table 2 summarizes the audiovestibular features of the patients with *DNFA5* mutations reported thus far (Van Laer et al., 1998; Yu et al., 2003; Bischoff et al., 2004; Cheng et al., 2007; Park et al., 2010). The age of onset of HL varied from the first to the fifth decade. Therefore, a 22-year-old female (V:10) in the TMDU244 family who showed normal hearing in the presence of the mutation may develop HL in the future. It has been reported that HL starts at high frequencies and progresses with additional deterioration of the middle and lower

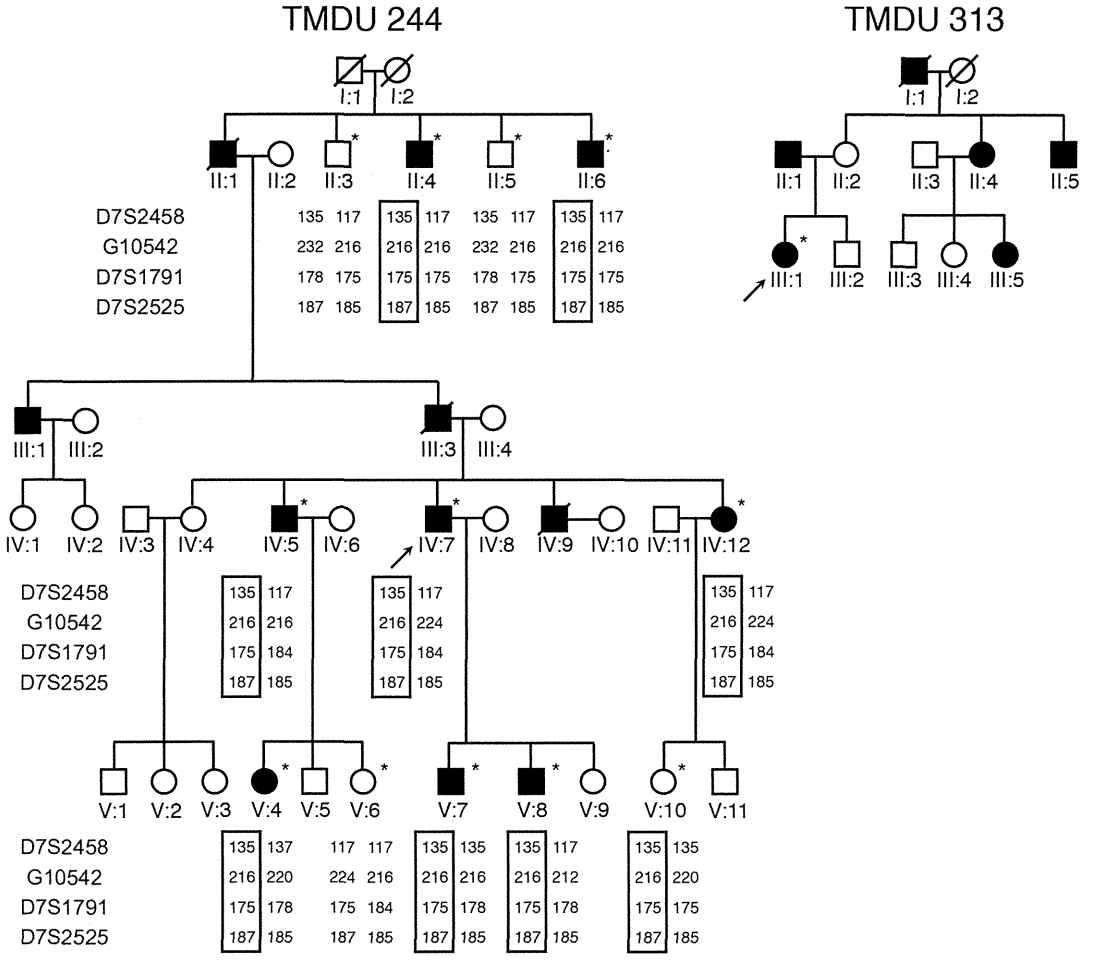

Figure 2 Pedigrees of families TMDU 244 and TMDU 313. For the TMDU 244 family, microsatellite marker haplotypes are shown with the DFNA5-linked haplotype in boxes. Individual V:10 with normal hearing carries the mutation. *; Family members in whom pure-tone audiometry and genetic analysis were available.

frequencies (Van Laer et al., 1998; Yu et al., 2003; Bischoff et al., 2004; Cheng et al., 2007; Park et al., 2010);tinnitus can be accompanied by HL (Cheng et al., 2007), word recognition is relatively good, with a score of >50% (Van Laer et al., 1998; De Leenheer et al., 2002; Bischoff et al., 2004), and no DFNA5 patients suffer from vestibular symptoms. These audiovestibular features of DFNA5 are consistent with those observed in our DFNA5 families. Although previous reports have found no spontaneous nystagmus and/or abnormal caloric responses, two members in the TMDU244 family showed positional nystagmus and/or caloric hypoplexia, suggesting that the *DFNA5* mutation causes mild vestibular impairment.

In this study, we analyzed the limited region of exons 7–9 and introns 6–8 of *DFNA5* in Japanese NSHHL patients. However, the region included introns 7 and 8, where all four reported mutations are located (Van Laer et al., 1998; Yu et al., 2003; Bischoff et al., 2004; Cheng et al., 2007). These mutations are expected to lead to skipping of exon 8 with a frameshift, which is thought to cause premature truncation of the DFNA5 protein and HL due to a gain-of-function. Therefore, the region between introns 7 and 8 is critical and should be screened for autosomal dominant NSHHL. The prevalence of *DFNA5* mutations among Japanese autosomal dominant NSHHL families is estimated to be >3% (2/65).

We detected 24 known polymorphisms in 65 Japanese NSHHL patients. The allele frequencies were consistent with those reported in the Japanese HapMap and 1000 Genomes data. The other 13 variants were not found in these databases, although they were detected in 100 Japanese healthy controls and are therefore considered to be polymorphisms.

Table 1 Haplotype analysis of DFNA5 families.

Nucleotide variations	SNP/STR marker	Distance to c.991-15_991-13del (bp)	Linked allele			Genotype TMDU313	Allele frequency[1] (Japanese)
			Korean[2]	Chinese[2]	TMDU244		
(CA)n	D7S2525	745,871	185	185	187	187/185	NA
(ATA)n	D7S1791	396,627	175	157	175	175/160	NA
c.1200 A > G	rs17149912	3573	A	G	G	G/G	A 0.674
c.1184-101 G > A	rs2240005	3456	G	G	G	G/G	G 0.722
c.1184-133 T > C	rs2074142	3424	T	T	T	T/T	T 0.721
c.1184-753 G > C	rs4719777	2804	C	C	C	C/C	G 0.422
c.991-15_991-13		0	del	del	del	del/WT	NA
c.991-27 A > G	rs2269812	13	A	A	A	G/G	A 0.837
c.991-31 C > T	rs17209408	17	C	C	C	C/C	C 1.000
c.991-67 G > A	rs57866118	53	G	G	G	G/G	G 0.942
c.991-70 C > G	rs55980618	56	C	C	C	C/C	NA
c.862+1393 G > A	rs2240006	2441	G	G	G	G/G	G 0.758
c.862+813 ins/del (A)	rs59938883	3022	del	del	del	del/del	NA
c.862+644 G > T	rs17149943	3190	G	G	G	G/T	G 0.813
c.862+87 ins/del (C)	rs35529766	3747	del	del	del	del/ins	NA
c.619 G > A	rs12540919	10,942	G	G	G	G/G	G 0.866
c.489 G > A	rs754555	12,744	A	A	A	A/G	G 0.535
c.447 A > G	rs876305	12,786	G	G	G	G/G	A 0.006
c.424 C > A	rs754554	12,809	A	A	A	A/C	C 0.541
c.405-15 G > A	rs754553	12,843	A	A	A	A/G	G 0.535
c.212-30 C > T	rs2521768	38,394	T	T	T	T/T	C 0.314
c.212-54 G > A	rs55926631	38,418	G	G	G	G/G	NA
c.-19-36 C > T	rs10235527	43,440	T	C	T	T/T	C 0.780
(GATA)n	G10542	1,607,773	220	212	216	216/216	NA
(CA)n	D7S2458	2,654,733	131	131	135	135/117	NA

[1]Allele frequency for each SNP is obtained from the HapMap or 1000 Genomes.
[2]Linked alleles in Korean and Chinese patients are given from a previous report by Park et al. (2010).
NA, not available; SNP, single-nucleotide polymorphism; STR, short tandem repeat; WT, wild type.

Park et al. (2010) compared the c.991-15_991-13del mutation-linked haplotypes between the Chinese and Korean families and suggested that the 3 bp deletion mutation showed a possible founder effect in East Asians. In the present study, we analyzed and compared the mutation-linked haplotypes in the Japanese family with those observed in the Chinese and Korean families. The DFNA5-linked haplotypes shared an identical region of 41,874 bp spanning from rs2240005 to rs55926631. These findings strongly suggest that the 3 bp deletion mutation was derived from an ancestor with NSHHL, exhibiting a founder effect in East Asians. In addition, the genotypes in the TMDU313 patient were identical to the TMDU244-linked haplotypes in a broad region of 3,400,604 bp spanning from D7S2525 to D7S2458, with the exception of the A > G variant (rs2269812). The TMDU313 patient was homozygous for the G allele, thus implying that a mutation had occurred in one of her ancestors. Possible mechanisms of the A > G variant are as follows: 1) a point mutation; 2) gene conversion; or 3) double equal crossing over, although it is unlikely that double equal crossing over occurred in a short stretch of 16 bp between the 3 bp deletion mutation and rs17209408. Furthermore, the LD structure obtained from the HapMap data for Japanese and Chinese showed a strong LD block containing the whole *DFNA5* gene as well as *MPP6* and a part of *OSBPL3*. The finding suggests that the recombination of SNPs and microsatellite markers found among the DFNA5-linked haplotypes in Chinese, Korean, and Japanese NSHHL families is not due to the existence of a recombination hotspot within the *DFNA5* locus.

A mouse mutant with a targeted deletion of exon 8 of *Dfna5* did not display HL, thus suggesting that haploinsufficiency is not responsible for the DFNA5-associated HL (Van Laer et al., 2005). Light microscopic findings show that the

Table 2 Clinical features of patients with DFNA5 mutations.

Family origin	Mutation	Location	Mutation effect	Onset age (y.o.)	HL progression	Tinnitus	AG	HL degree (dBHL)	WRS (%)	Vestibular symptom	Vestibular function	Reference
Dutch	c.990+503_990+1691 del ins132	Intron 7	Skipping of exon 8	10–22	+	−	HF	80 above 1000 Hz	50–100	−		(Van Laer et al., 1998)
Chinese	c.991-15_991-13del	Intron 7	Skipping of exon 8	7–30	+		HF	60–100				(Yu et al., 2003)
Dutch	c.991-6C > G	Intron 7	Skipping of exon 8	28–49	+		HF	30–90	50–100	−	Normal	(Bischoff et al., 2004)
Chinese	c.1183+4A > G	Intron 8	Skipping of exon 8	11–50	+	+	HF	50–90		−		(Cheng et al., 2007)
Korean	c.991-15_991-13del	Intron 7	Skipping of exon 8	10–19	+		HF	30–100		−		(Park et al., 2010)
Japanese	c.991-15_991-13del	Intron 7	Skipping of exon 8	10–30	+	+	HF	30–100		−	Caloric Hypoplexia	This study
Japanese	c.991-15_991-13del	Intron 7	Skipping of exon 8	18	+	+	HF	50–70	80	−		This study

HL, hearing loss; AG, audiogram; WRS, word recognition score; HF, high frequency.

Dfna5$^{-/-}$ mouse has a normal structure in the middle and inner ear, and no differences are observed between *Dfna5*$^{-/-}$ and *Dfna5*$^{+/+}$ mice in the organ of Corti or the cochlear ganglion cells. However, scanning electron microscopy findings demonstrate significant differences in the number of fourth row outer hair cells between *Dfna5*$^{-/-}$ and *Dfna5*$^{+/+}$ mice. On the other hand, yeast cells tolerate the expression of wild-type *DFNA5*, while the expression of the mutant *DFNA5* allele leads to cell cycle arrest (Gregan et al., 2003). The post-transfection death of mammalian cells approximately doubles when the cells are transfected with mutant *DFNA5*–GFP compared with wild-type *DFNA5*–GFP (Van Laer et al., 2004). These experiments support the hypothesis that the hearing impairment associated with *DFNA5* is caused by a "gain-of-function" mutation and that the mutant *DFNA5* has a deleterious new function.

DFNA5 has also been identified as a transcriptional target of P53 and is suggested to be a tumor suppressor gene (Masuda et al., 2006). The transfection of mutant *DFNA5* leads to cell death in mammalian cells (Op de Beeck et al., 2011a, b, 2012), thus suggesting that *DFNA5* mutations induce apoptosis. An analysis of the DFNA5 protein revealed two separated regions (Op de Beeck et al., 2011a). The first region, which includes exon 2 to exon 6, induces apoptosis, whereas the second region, which includes exon 8, has a regulatory function (Op de Beeck et al., 2011a). The skipping of exon 8 could shorten the second region, thus leaving the apoptosis-inducing region uncovered, and resulting in a constitutively activated mutant protein that may induce apoptosis (Op de Beeck et al., 2011a). The presence of HL in DFNA5 patients is considered to be the result of an activating mutation (Op de Beeck et al., 2012). It is implied that the apoptosis-inducing feature of mutant *DFNA5* may cause continued stress on cells of the sensory epithelium (Op de Beeck et al., 2012).

In summary, we identified the previously identified 3 bp deletion mutation in *DFNA5* in two of 65 Japanese patients with autosomal dominant NSHHL. An analysis of the DFNA5-linked haplotypes in Japanese patients suggested that this mutation was derived from the same ancestor in the Chinese, Korean, and Japanese DFNA5 families.

Acknowledgements

We sincerely thank the families for their participation in this study. This work was supported by JSPS KAKENHI Grant Numbers 24791754, 22659305, 23390399, and 21390459, and by a grant-in-aid for scientific research from the Ministry of Health, Labor and Welfare of Japan (H23-kankaku-005).

Conflict of Interest

The authors have no conflicts of interest to declare.

References

Bischoff, A. M., Luijendijk, M. W., Huygen, P. L., van Duijnhoven, G., De Leenheer, E. M., Oudesluijs, G. G., Van Laer, L., Cremers, F. P., Cremers, C. W. & Kremer, H. (2004) A novel mutation identified in the DFNA5 gene in a Dutch family: a clinical and genetic evaluation. *Audiol Neurootol* **9**, 34–46.

Cheng, J., Han, D. Y., Dai, P., Sun, H. J., Tao, R., Sun, Q., Yan, D., Qin, W., Wang, H. Y., Ouyang, X. M., Yang, S. Z., Cao, J. Y., Feng, G. Y., Du, L. L., Zhang, Y. Z., Zhai, S. Q., Yang, W. Y., Liu, X. Z., He, L. & Yuan, H. J. (2007) A novel DFNA5 mutation, IVS8+4 A>G, in the splice donor site of intron 8 causes late-onset non-syndromic hearing loss in a Chinese family. *Clin Genet* **72**, 471–477.

De Leenheer, E. M., van Zuijlen, D. A., Van Laer, L., Van Camp, G., Huygen, P. L., Huizing, E. H. & Cremers, C. W. (2002) Further delineation of the *DFNA5* phenotype: result of speech recognition tests. *Ann Otol Rhinol Laryngol* **111**, 639–641.

Gregan, J., Van Laer, L., Lieto, L. D., Van Camp, G. & Kearsey, S. E. (2003) A yeast model for the study of human DFNA5, a gene mutated in nonsyndromic hearing impairment. *Biochim Biophys Acta* **1638**, 179–186.

Hilgert, N., Smith, R. J. & Van Camp, G. (2009) Function and expression pattern of nonsyndromic deafness genes. *Curr Mol Med* **9**, 546–564.

Ito, T., Noguchi, Y., Yashima, T., Ohno, K. & Kitamura, K. (2010) Hereditary hearing loss and deafness genes in Japan. *J Med Dent Sci* **57**, 1–10.

Korver, A. M., Admiraal, R. J., Kant, S. G., Dekker, F. W., Wever, C. C., Kunst, H. P., Frijns, J. H., Oudesluys-Murphy, A. M. & DECIBEL-collaborative study group. (2011) Causes of permanent childhood hearing impairment. *Laryngoscope* **121**, 409–416.

Masuda, Y., Futamura, M., Kamino, H., Nakamura, Y., Kitamura, N., Ohnishi, S., Miyamoto, Y., Ichikawa, H., Ohta, T., Ohki, M., Kiyono, T., Egami, H., Baba, H. & Arakawa, H. (2006) The potential role of DFNA5, a hearing impairment gene, in p53-mediated cellular response to DNA damage. *J Hum Genet* **51**, 652–664.

Mazzoli, M., Van Camp, G., Newton, V., Giarbini, N., Declau, F. & Parving, A. (2003) Recommendations for the description of genetic and audiological data for families with non-syndromic hereditary hearing impairment. *Audiol Med* **1**, 148–150.

Morton, C. C. & Nance, W. E. (2006) Newborn hearing screening—a silent revolution. *N Eng J Med* **354**, 2151–2164.

Op de Beeck, K., Van Camp, G., Thys, S., Cools, N., Callebaut, I., Vrijens, K., Van Nassauw, L., Van Tendeloo, V. F., Timmermans, J. P. & Van Laer, L. (2011a) The *DFNA5* gene, responsible for hearing loss and involved in cancer, encodes a novel apoptosis-inducing protein. *Eur J Hum Genet* **19**, 965–973.

Op de Beeck, K., Schact, J. & Van Camp, G. (2011b) Apoptosis in acquired and genetic hearing impairment: the programmed death of the hair cell. *Hear Res* **281**, 18–27.

Op de Beeck, K., Van Laer, L. & Van Camp, G. (2012) *DFNA5*, a gene involved in hearing loss and cancer: a review. *Ann Otol Rhinol Laryngol.* **121**, 197–207.

Park, H. J., Cho, H. J., Baek, J. I., Ben-Yosef, T., Kwon, T. J., Griffith, A. J. & Kim, U. K. (2010) Evidence for a founder mutation causing DFNA5 hearing loss in East Asians. *J Hum Genet* **55**, 59–62.

Van Camp, G., Coucke, P., Balemans, W., Van Velzen, D., Van de Bilt, C., Van Laer, L., Smith, R. J., Fukushima, K., Padberg, G. W., Frants, R. R., Van de Heyning, P., Smith, S. D., Huzing, E. H. & Willems, P. J. (1995) Localization of a gene for non-syndromic hearing loss (DFNA5) to chromosome 7p15. *Hum Mol Genet* **4**, 2159–2163.

Van Camp, G., Willems, P. J. & Smith, R. J. (1997) Nonsyndromic hearing impairment: Unparalleled heterogeneity. *Am J Hum Genet* **60**, 758–764.

Van Laer, L., Huizing, E. H., Verstreken, M., van Zuijlen, D., Wauters, J. G., Bossuyt, P. J., Van de Heyning, P., McGuirt, W. T., Smith, R. J., Willems, P. J., Legan, P. K., Richardson, G. P. & Van Camp, G. (1998) Nonsyndromic hearing impairment is associated with a mutation in DFNA5. *Nat Genet* **20**, 194–197.

Van Laer, L., Meyer, N. C., Malekpour, M., Riazalhosseini, Y., Moghannibashi, M., Kahrizi, K., Vandevelde, A., Alasti, F., Najmabadi, H., Van Camp, G. & Smith, R. J. (2007) A novel DFNA5 mutation does not cause hearing loss in an Iranian family. *J Hum Genet* **52**, 549–552.

Van Laer, L., Pfister, M., Thys, S., Vrijens, K., Mueller, M., Umans, L., Serneels, L., Van Nassauw, L., Kooy, F., Smith, R. J., Timmermans, J. P., Van Leuven, F. & Van Camp, G. (2005) Mice lacking Dfna5 show a diverging number of cochlear fourth row outer hair cells. *Neurobiol Dis* **19**, 386–399.

Van Laer, L., Vrijens, K., Thys, S., Van Tendeloo, V. F., Smith, R. J., Van Bockstaele, D. R., Timmermans, J. P. & Van Camp, G. (2004) DFNA5: Hearing impairment exon instead of hearing impairment gene? *J Med Genet* **41**, 401–406.

Yu, C., Meng, X., Zhang, S., Zhao, G., Hu, L. & Kong, X. (2003) A 3-nucleotide deletion in the polypyrimidine tract of intron 7 of the DFNA5 gene causes nonsyndromic hearing impairment in a Chinese family. *Genomics* **82**, 575–579.

Supporting Information

Additional Supporting Information may be found in the online version of this article:

Table S1 Nucleotide sequences of primers for PCR, sequencing and microsatellite analyses used in this study.

Table S2 Novel polymorphisms of DFNA5 found in this study.

Figure S1 Pure-tone audiograms of nine members of the TMDU244 family and the proband of the TMDU313 family.

Audiograms obtained from subjects carrying the *DFNA5* mutation are shown. The *X*-axis shows the stimulus frequency (Hz) and the *Y*-axis indicates the hearing threshold (dB HL). All members, except for TMDU313 V:10, show bilateral symmetrical high-frequency sensorineural hearing loss.

Figure S2 LD structure of the region around *DFNA5*. The LD structure was investigated using the HapMap data for Japanese (JPT) and Chinese (CHB). The upper panel shows the LD for the JPT data, while the lower panel shows the LD for the CHB data. Each panel contains the LD structure derived from data for r^2 and D'. LD blocks, from block A to block G, deduced from the r^2 plot data are indicated by red arrows. The name and transcriptional direction (blue dotted arrows) are shown for each gene. The telomere and centromere sides are indicated at the most upper part. The scale bar represented by a black arrow in the map indicates 100 kb.

Received: 13 November 2013
Accepted: 16 December 2013

Audiology Japan 57, 63～70, 2014

軽度難聴の急性感音難聴症例の検討

野口佳裕，籾山直子，高橋正時，喜多村　健
東京医科歯科大学耳鼻咽喉科

要旨：本研究では，原因不明に発症し，５周波数平均聴力レベルが40dB未満の軽度の急性感音難聴症例37例（年齢22～78歳；男性20例，女性17例）を検討した。急性低音障害型感音難聴症例は除外した。患者を隣り合う３周波数の聴力レベルが30dB HL以上のＡ群とそれ以外のＢ群に分類した。難聴はＡ群の70%，Ｂ群の79%が自覚し，耳鳴はＡ群の91%，Ｂ群の92%に認められた。最も頻度の高い聴力型は，両群とも高音障害型であった。めまいはＡ群の26%，Ｂ群の14%に随伴したが，頭位眼振検査ではＡ群の56%，Ｂ群の36%に定方向性眼振が認められた。聴力予後は全症例の51%が「不変」を示し，軽度の急性感音難聴の予後は必ずしも良好ではなかった。今後，本邦ではこれまで突発性難聴から除外されてきた可能性のある軽度の急性感音難聴の病態を，十分に検討していく必要があると考えられた。

ーキーワードー
軽度難聴，急性感音難聴，突発性難聴，めまい，眼振

はじめに

突発性難聴は，突然に通常一側に生じる原因不明の感音難聴である。欧米で一般的に使用される診断基準には「隣り合う３周波数の聴力レベルが30dB以上」とする聴力レベルに関する規定がある[1]。一方，本邦では昭和48年に作成された突発性難聴診断の手引[2]において，難聴の程度については「必ずしも高度である必要はないが，実際問題としては高度でないと突然難聴になったことに気付かないことが多い」と付記されているものの，主症状の１つとして「難聴の性質は高度の感音難聴である」ことが明記されている。このため，高度難聴を示さない突然生じた感音難聴の診断を突発性難聴とするか否かは担当医師の裁量に委ねられ，一部の症例において診断上の混乱が生じていた可能性は否定できない。

近年，厚生労働省特定疾患急性高度難聴調査研究班では，突発性難聴の診断基準（案）（2012年改訂）（以下，新基準案）（表１）を作成した[3]。新基準案では欧米の診断規準との整合性を加味し，参考事項として難聴が「隣り合う３周波数で各30dB以上」であることが明記されている。今回我々は，従来の本邦の診断基準では突発性難聴から除外されていた可能性のある軽度難聴の急性感音難聴を検討した。

対象と方法

2005年１月から2009年12月の間に当科難聴・耳鳴・補聴器外来を受診した軽度難聴の急性感音難聴症例37例を対象とし，診療録より後方視的に検討した。性別は男性20例，女性17例であり，年齢は22～78歳（平均年齢47.1±14.0歳）であった。軽度難聴の急性感音難聴の診断基準は，1)急性あるいは突発性に難聴，耳鳴が発症，2)平均聴力レベルが40dB未満，3)原因不明のすべてをみたすものとした。ここで，平均聴力レベルは周波数250，500，1000，2000，4000Hzの５周波数平均聴力レベル（以下，

表1 突発性難聴の診断基準（案）（厚生労働省特定疾患急性高度難聴調査研究班2012年改訂）

主症状

1．突然発症
2．高度感音難聴
3．原因不明

参考事項

1．難聴（参考：隣り合う3周波数で各30dB以上の難聴）
(1) 文字どおり即時的な難聴，または朝，目が覚めて気づくような難聴が多いが，数日をかけて悪化する例もある。
(2) 難聴の改善・悪化の繰り返しはない。
(3) 一側性の場合が多いが，両側性に同時罹患する例もある。
2．耳鳴
難聴の発生と前後して耳鳴を生じることがある。
3．めまい，および吐気・嘔吐
難聴の発生と前後してめまい，および吐気・嘔吐を伴うことがあるが，めまい発作を繰り返すことはない。
4．第8脳神経以外に顕著な神経症状を伴うことはない。

診断の基準：主症状の全事項をみたすもの

表2 突発性難聴・聴力回復の判定基準（急性高度難聴調査研究班1984年改正）

治癒（全治）
1．250，500，1000，2000，4000Hzの聴力レベルが20dB以内にもどったもの
2．健側聴力が安定と考えられれば，患側がそれと同程度まで改善したとき

著明回復
上記5周波数の算術平均値が30dB以上改善したとき

回復（軽度回復）
上記5周波数の算術平均値が10–30dB未満改善したとき

不変（悪化を含む）
同じくの値が10dB未満の変化

平均聴力レベル）とした。また，非罹患耳の聴力は正常もしくは年齢相応を示し，発症後2週間までの間に当科もしくは前医を受診し，前医からの紹介例については前医での初診時オージオグラムが判明しているもののみを対象とした。除外診断は，(1)急性低音障害型感音難聴診断基準（案）（厚生労働省特定疾患急性高度難聴調査研究班，2012年改訂）をみたす例，(2)難聴発症後数日以降に平均聴力レベルが10dB以上悪化もしくは変動する例とした。

対象を「隣り合う3周波数で各30dB以上の難聴」をみたし新基準案にて突発性難聴（重症度分類Grade 1）に分類される23例（A群）と，「30dB以上の難聴を示す周波数が2周波数以下」あるいは「30dB以上の難聴が3周波数以上あるが隣り合わない」などの理由で新基準案をみたさない14例（B群）に分類した。検討項目は，年齢，性別，罹患耳と非罹患耳の聴力レベル（平均聴力レベル，周波数別聴力レベル），発症時の聴平衡覚症状（難聴，耳鳴，めまいなど）の有無，聴力型，眼振所見，聴力予後とした。聴力型は，当科もしくは前医初診時のオージオグラムを神崎らの報告[4]に従い分類した。眼振は，当科初診時において赤外線CCDカメラもしくはフレンツェル眼鏡を用いた頭位眼振検査により評価した。聴力予後判定は，発症後3カ月以上経過して聴力が固定したと考えられる時点において，突発性難聴・聴力回復の判定基準（1984年改正）（表

2)[5]に基づき行った。

治療は36例が発症後7日以内に開始されていたが，1例は8日目より行われていた。薬物治療として副腎皮質ステロイド剤（以下，ステロイド）が32例（86%），ATP・ビタミンB_{12}製剤が37例（100%），プロスタグランディンE_1製剤が9例（24%）に行われ，星状神経節ブロックが5例（14%），高気圧酸素治療が18例（49%）に施行されていた。また，プレドニゾロン，ハイドロコルチゾン，ベタメタゾン，デキサメタゾンなどの種類の異なるステロイドが症例ごとに使用されていた。

統計処理はJMPバージョン9.0.2（SAS Institute Inc.）を用いPearsonのχ^2検定もしくはWilcoxonの順位和検定にて行い，$p<0.05$を有意差ありとした。

結　果

1．各群の年齢分布，性別，平均聴力レベル

各群の年齢分布を図1に示した。全症例でみると30代と50代に二峰性のピークを認めたが，A群のみをみると50代にピークをもつ山型を示した。一方，B群では60歳以上の症例は認められなかった。

平均年齢，性別，罹患耳・非罹患耳の平均聴力レベル・各周波数の聴力レベルを表3に示した。平均年齢はA群の方がB群より高かったが，有意差は認められなかった。性別はA群では男性，B群では女性の割合が多い傾向を認めたが，男女比に有意差は認められなかった。平均聴力レベルは，罹患耳，非罹患耳ともにB群に比べA群で有意に高値を示し

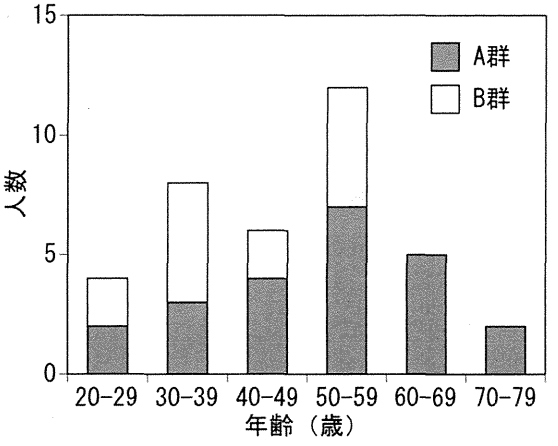

図1　年齢分布

表3　全症例，A群，B群のプロファイル

		全症例	A群	B群	p
平均年齢（歳）		47.1±14.0	50.4±14.1	41.5±12.5	0.0601
性別（男：女）		20：17	15：8	5：9	0.0807
罹患耳 平均聴力レベル（dB）		4～39 （平均28.0±8.6）	23～39 （平均33.1±4.1）	4～26 （平均19.6±7.2）	<0.05
非罹患耳 平均聴力レベル（dB）		3～21 （平均12.2±5.0）	7～21dB （平均14.1±4.0）	3～21dB （平均9.1±5.0）	<0.05
罹患耳 聴力レベル （dB）	125Hz	21.9±7.5	23.2±8.2	20.0±5.9	0.2303
	250Hz	24.3±9.8	27.4±9.2	19.3±8.7	<0.05
	500Hz	24.1±9.2	27.8±8.8	17.9±6.1	<0.05
	1000Hz	24.2±11.5	29.6±9.6	15.4±8.7	<0.05
	2000Hz	30.1±11.2	35.4±7.7	21.4±10.8	<0.05
	4000Hz	37.3±18.7	45.4±12.1	23.9±20.3	<0.05
	8000Hz	52.7±21.3	58.7±15.2	42.9±26.5	0.0822
非罹患耳 聴力レベル （dB）	125Hz	17.6±5.4	19.6±4.7	14.3±4.7	<0.05
	250Hz	15.8±5.7	17.8±4.5	12.5±6.1	<0.05
	500Hz	12.6±6.7	13.5±5.1	11.1±8.8	<0.05
	1000Hz	10.0±6.3	12.2±5.8	6.4±5.7	<0.05
	2000Hz	11.6±8.0	13.9±8.7	7.9±5.1	<0.05
	4000Hz	10.9±8.1	13.0±7.5	12.1±12.4	<0.05
	8000Hz	19.6±14.6	24.1±14.3	9.1±5.0	<0.05

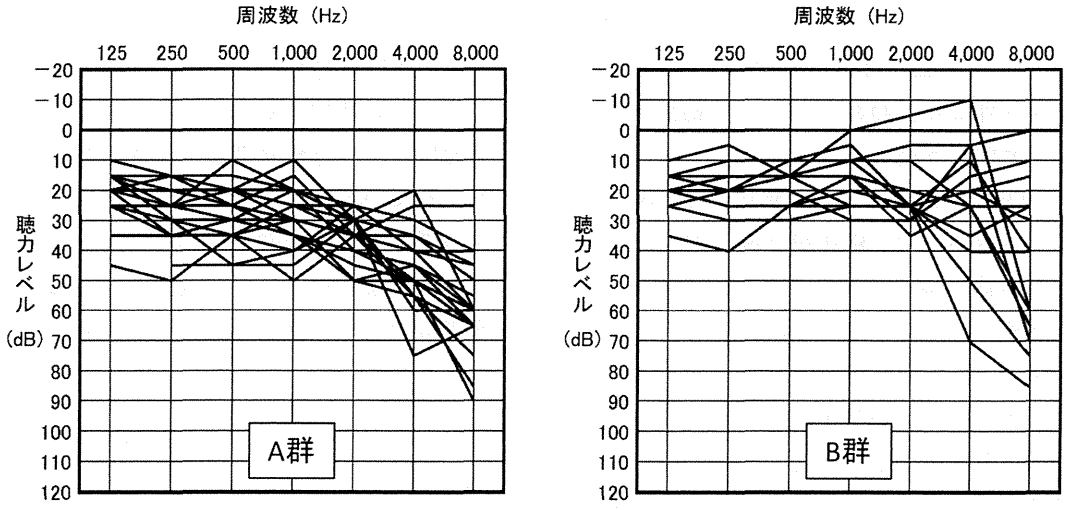

図2 A群，B群の重ね合わせオージオグラム

た。各周波数別の聴力レベルをみても，罹患耳，非罹患耳とも全ての周波数でB群よりもA群で高値を示し，統計学的には罹患耳の周波数125，8000Hzの聴力レベルを除き各群間に有意差を認めた。

2．聴覚症状

発症時の聴覚症状として，全症例37例中27例（73%）が難聴を自覚し，耳鳴は病歴聴取を行っていた35例中32例（91%）に認められた。その他の聴覚症状として，耳閉感を19例，聴覚過敏を9例に認めたが，診療録上これらの症状の有無が記載されていないものも多くみられたため，正確な頻度の判定はできなかった。

群別にみると，難聴はA群の70%（16/23），B群の79%（11/14）に存在し，耳鳴はA群の91%（20/22），B群の92%（12/13）に認められた。難聴，耳鳴の有無について，各群の間に有意差は認められなかった（難聴：$p=0.5497$，耳鳴：$p=0.8864$）。

3．オージオグラムと聴力型

A群とB群の各重ね合わせオージオグラムを図2に，聴力型ごとの症例数を表4に示した。全症例における聴力型は高音急墜型，高音漸傾型を示す症例が多く，これらを合わせた高音障害型は62%（23/37）を占めた。

各群でみると，A群の70%（16/23）は高音障害型を示したが，高音急墜型よりも高音漸傾型を示す例が軽度多く認められた。一方，B群では高音急墜型の次に谷型の例が多く，高音漸傾型を示す例は2例のみであった。このため，全体として高音障害型の割合は50%とA群よりも低くなった。しかし，各聴力型の有無に対して各群の間に有意差は認められなかった。

表4 全症例，A群，B群の聴力型と人数

	全症例（%）	A群	B群	p
高音急墜	12(32%)	7	5	0.7394
高音漸傾	11(30%)	9	2	0.1733
谷	6(16%)	2	4	0.1117
水平	4(11%)	2	2	0.5954
山	3(8%)	2	1	0.8667
低音障害	1(3%)	1	0	0.4290

4．前庭症状と眼振所見

初発時に浮動性もしくは回転性めまいを自覚した症例は，全症例の22%（8/37）であった。群別にみるとA群では26%（6/23），B群では14%（2/14）とA群にめまい症状を多く認めた。しかし，統計学的な有意差はなかった（$p=0.3977$）。

眼振検査は37例中27例に施行されており，眼振を認めた頻度は全症例の48%（13/27）であった。眼振は，全て定方向性の水平性もしくは水平性回旋性混合性眼振であり，9例が患側向き眼振，4例が健側向き眼振であった。眼振検査が施行された病日と眼振所見の関係をみると，第7病日までに検査を施行された18例中9例に眼振を認め，その中の7例が患側向き眼振であった（図3）。一方，第8病日以降に観察した9例中4例に眼振を認め，患側向き眼振と健側向き眼振はそれぞれ2例に認められた。群